Short Communication

Electrodeposition of Ni-Mo/TiO$_2$ Nanocomposite Coatings on Low-Carbon Steels for Improving Corrosion Resistance

Xinjing Meng[1], Xiaofen Wang[2,], Derong Zhang[2], Hao Luo[2], Chenhua Xu[1], Songli Liu [3,*]*

[1]Shanghai University of Electric Power, Shanghai Engineering Research Center of Heat-exchange System and Energy Saving, Shanghai 200090, China
[2] School of Materials Science and Energy Engineering, Foshan University, Foshan 528000, China
[3]College of Materials Science and Engineering, Yangtze Normal University, Chongqing 408100, PR China
[*]E-mail: mengxinjing@shiep.edu.cn; wangwangxiaofen@126.com; pzhlsll@163.com

In this paper, Ni-Mo/TiO$_2$ nanocomposite coatings were successfully deposited from a modified ammonia-citrate bath containing TiO$_2$ nanoparticles. Phase identifications and microstructural characterizations of the as-prepared coatings were obtained by X-ray diffraction (XRD) and scanning electron microscopy (SEM). The corrosion behaviour was evaluated by a potentiodynamic polarization test and electrochemical impedance spectroscopy (EIS). It is established that the compact, crack-free Ni-Mo/TiO$_2$ nanocomposite coatings are composed of a Ni-Mo alloy matrix and a TiO$_2$ phase, and both the content of Mo and TiO$_2$ in the obtained composite coatings increase with an increased addition of TiO$_2$ in the plating bath. The Ni-Mo/TiO$_2$ nanocomposite coatings exhibit much nobler E_{corr}, lower i_{corr} and larger R_{ct} values than those of the Ni-Mo alloy coating. Among all Ni-Mo/TiO$_2$ nanocomposite coatings, the Ni-Mo/TiO$_2$ IV coating, deposited from a bath containing 40 mg/L TiO$_2$ nanoparticles, shows the best corrosion resistance.

1. INTRODUCTION

Electrodeposited hard chromium coatings are widely used in industry for improving the corrosion and wear resistance of many substrate metals (such as low-carbon steel and copper pipes) [1, 2]. However, its application is opposed by governments and environmental protection departments because of the toxicological and environmental restrictions of hard chromium use in industry [3]. Therefore, exploiting and applying alternative coatings, which are environmentally friendly and possess comparable performance with hard chromium coatings, have attracted increasing attention [4-6].

Metals in group VIB (molybdenum and tungsten), which exhibit high hardness and excellent corrosion resistance, have been demonstrated as potential candidates to replace hard chromium as a protective coating [7]. Molybdenum cannot be electrodeposited from aqueous solutions, but they can be induced by co-deposition with iron group metals to form alloy coatings (such as Fe-Mo, Co-Mo, Ni-Mo, and Ni-Fe-Mo) [8-10]. Among them, the Ni–Mo alloys are promising materials due to their high catalytic activity towards the hydrogen evolution reaction (HER) and their corrosion resistance [11, 12].

Electrodeposited nanocomposite coatings have become hot research topics because the second-phase reinforcing nanoparticles can greatly enhance the intrinsic performances or give extra specific characteristics [13-15]. Recently, a number of nanoparticles, such as ZrO_2 [11], Al_2O_3 [12], montmorillonite [13], and graphene oxide [15], have been incorporated into the Ni-Mo alloy matrix as a strengthening phase for better mechanical properties and corrosion resistance. TiO_2, a typical and superior ceramic material, has been used as reinforcing particles to improve the wear and corrosion resistance of electrodeposited coatings (e.g., Zn [15], Ni [16], Ni-Co [17], Ni-W [18], Ni-P [19], etc.). However, few studies have been reported on TiO_2-reinforced Ni-Mo nanocomposite coatings. Thus, an investigation of incorporating TiO_2 particles into Ni-Mo to fabricate composite coatings is quite meaningful and necessary.

Because low-carbon steel is widely used as an engineering material and its application is limited by its relatively high chemical activity, various surface treatments and coating technologies have been employed to enhance its corrosion, of which an electroplated composite coating is a promising option [20-22]. Therefore, the present work focuses on the electrodeposition of a Ni-Mo/TiO_2 nanocomposite coating and finding the optimum preparation parameters. To the best of our knowledge, this is the first attempt to co-deposit Ni-Mo/TiO_2 nanocomposite coatings on the surface of low-carbon steels to improve its hardness and corrosion resistance.

2. EXPERIMENTAL

The Ni-Mo/TiO_2 nanocomposite coatings were electrodeposited from a modified ammonia-citrate bath containing different additions of TiO_2 nanoparticles, and the compositions of the plating baths are listed in Table 1. A direct current electrodeposition method was used in this paper, in which low-carbon steel (10 mm×10 mm) and a platinum sheet (20 mm×20 mm) were used as the cathode and anode, respectively. Operating parameters are listed in Table 1. All electroplating baths were prepared by analytical grade raw materials purchased from National Pharmaceutical and Reagent (China) and double distilled water.

Table 1. Compositions of the plating baths and the operating parameters

Plating baths	Operating parameters
$Na_2MoO_4 \cdot 2H_2O$: 40 g/L	Current density: 20 mA/cm^2
$NiSO_4 \cdot 6H_2O$: 130 g/L	Temperature (T): 60
$C_6H_5O_7(NH_4)_3$: 48 g/L	Stirring speed: moderate, ~100 r/min
$C_2H_5NO_2$: 6 g/L	pH (adjusted by $NH_3 \cdot H_2O$): 9.00±0.1
TiO_2 nanoparticles: 0, 10, 20, 30, 40, 50 mg/L, respectively.	

Coating morphologies were observed by scanning electron microscopy (SEM, SU5000, Hitachi) operating at 15 kV. Chemical compositions and distributions of the coating were investigated by using energy-dispersive spectroscopy (EDS, Oxford). Phase constitutions of the obtained coatings were characterized by X-ray diffraction (XRD, Empyrean XRD-Panalytical) with Cu Kα radiation (λ=1.5406 Å), operating at 40 kV and 40 mA and a scanning range from 10º to 80º with a step of 0.01º.

Corrosion behaviours were investigated by a potentiodynamic polarization test in conjunction with electrochemical impedance spectroscopy (EIS) by using an electrochemical workstation (CHI660E). The potentiodynamic polarization test was operated from -0.15 V to +0.15 V vs. the corrosion potential (E_{corr}), using a scan rate of 0.167 mV/s^{-1}. The EIS test was conducted at the open circuit potential (E_{cop}), with a voltage perturbation amplitude of 10 mV in a frequency range of 10^5 Hz to 10^{-2} Hz. The electrochemical tests were conducted in a conventional three-electrode cell (consisting of the deposited coating as the working electrode, a Pt sheet (20 mm×20 mm) as the counter electrode and an saturated calomel electrode (SCE) as the reference electrode). All experiments were carried out at room temperature (~25 °C) in 3.5 wt.% NaCl solution.
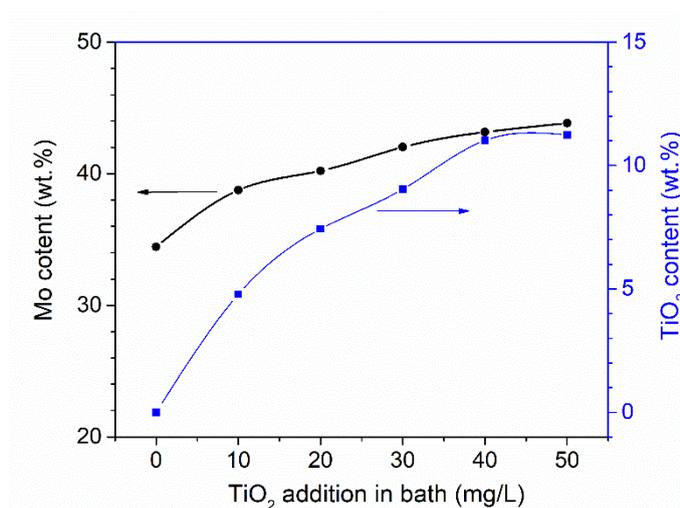
3. RESULTS AND DISCUSSION

Figure 1. Comparisons of the coatings deposited from baths containing different amounts of TiO$_2$ nanoparticles.

Fig. 1 shows the comparisons of the coatings deposited from baths containing different amounts of TiO$_2$ nanoparticles. It is established that both the Mo content and TiO$_2$ content increase as the TiO$_2$ addition increases in the plating baths. This phenomenon has been observed in previous studies on the electrodeposition of composite coatings and is attributed to the increased nanoparticles adsorbed on the cathode surface, which reduces the amount of nuclear energy [23-25]. In this paper, the obtained coatings (Ni-34.5 wt.%, Mo; Ni-38.8 wt.%, Mo-4.8 wt.%, TiO$_2$; Ni-40.2 wt.%, Mo-7.4 wt.%, TiO$_2$; Ni-42.0 wt.%, Mo-9.0 wt.%, TiO$_2$; Ni-43.2 wt.%, Mo-11.0 wt.%, TiO$_2$; and Ni-43.2 wt.% Mo-11.4 wt.% TiO$_2$) are

denoted as Ni-Mo, Ni-Mo/TiO$_2$ I, Ni-Mo/TiO$_2$ II, Ni-Mo/TiO$_2$ III, Ni-Mo/TiO$_2$ IV, Ni-Mo/TiO$_2$ V, respectively.
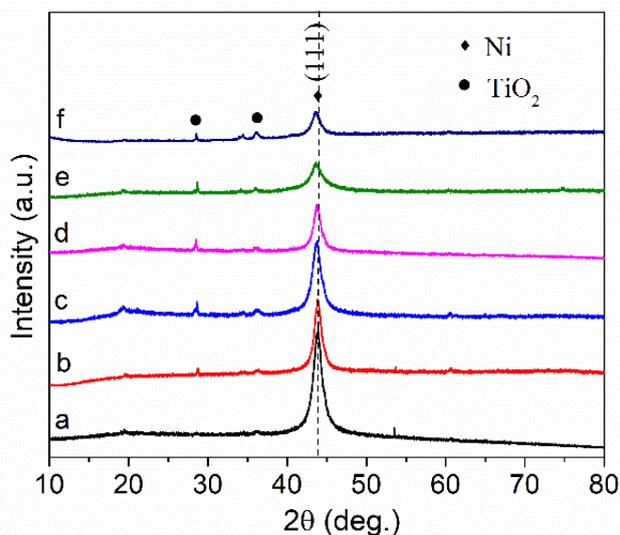

Figure 2. XRD patterns of the obtained Ni-Mo coating (a) and Ni-Mo/TiO$_2$ coatings (b: Ni-Mo/TiO$_2$ I, c: Ni-Mo/TiO$_2$ II, d: Ni-Mo/TiO$_2$ III, e: Ni-Mo/TiO$_2$ IV, and f: Ni-Mo/TiO$_2$ V)

Phase compositions of the electrodeposited coatings were determined by an XRD analysis. As shown in Fig. 2, the sharp, narrow peak at 2θ≈43.7° should correspond to the (1 1 1) plane of a face-centred cubic (FCC) Ni crystalline. It should be noted that this peak is at a slightly lower degree than that of the (1 1 1) reflection of pure Ni because the Mo atoms dissolve and substitute into the Ni lattice, which results in the lattice parameters of the Ni-Mo alloy becoming larger than that of pure Ni [26, 27]. In addition, the peak corresponding to the (1 1 1) plane shifts to a lower degree with an increased addition of TiO$_2$ nanoparticles in the plating baths due to the increased lattice parameters caused by increased Mo content in the electrodeposited coating (shown in Fig. 1). It can also be found that a TiO$_2$ phase (PDF 75-1749) exists for the coatings electrodeposited in the plating baths containing TiO$_2$ nanoparticles (10-50 mg/L), while no traces of the TiO$_2$ phase are detected for the coating obtained in the baths without TiO$_2$ nanoparticles (Fig. 1) [28]. The above results confirm that the TiO$_2$ nanoparticles are successfully introduced into the Ni-Mo alloy coating, which is consistent with the chemical composition results (Fig. 1).

Furthermore, the intensity of the (1 1 1) peak decreases with an increasing addition of TiO$_2$ nanoparticles. As reported in previous studies on the electrodeposition of a Ni-Mo alloy coating, TiO$_2$ nanoparticles can provide nucleated active sites and decrease the total energy of the system for crystal nucleation and growth [29-32]. Therefore, the (1 1 1) grains with a low energy density will decrease accordingly [25, 33].
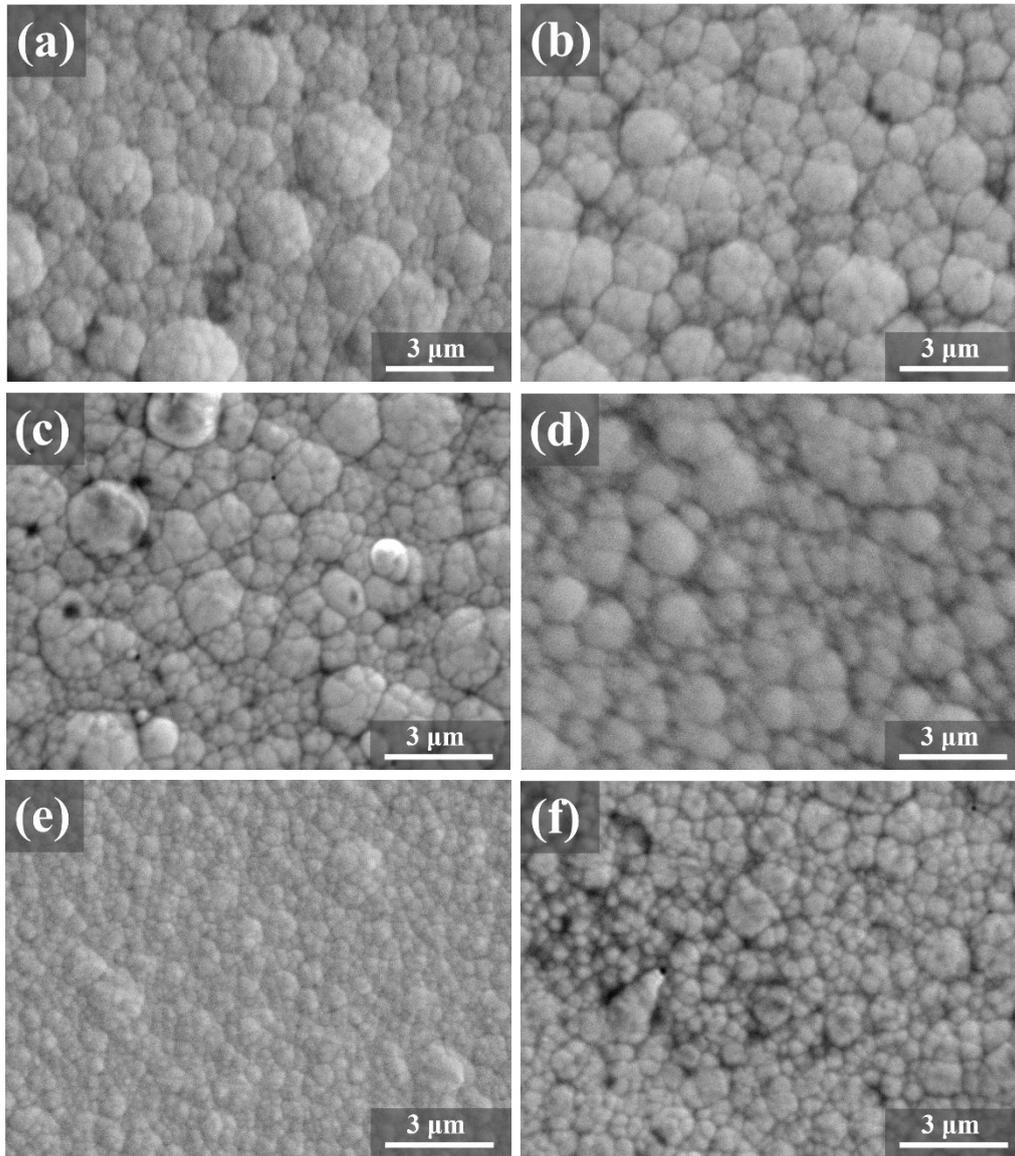
Figure 3. Surface morphologies of the obtained Ni-Mo coating (a) and Ni-Mo/TiO$_2$ coatings (b: Ni-Mo/TiO$_2$ I, c: Ni-Mo/TiO$_2$ II, d: Ni-Mo/TiO$_2$ III, e: Ni-Mo/TiO$_2$ IV, and f: Ni-Mo/TiO$_2$ V).
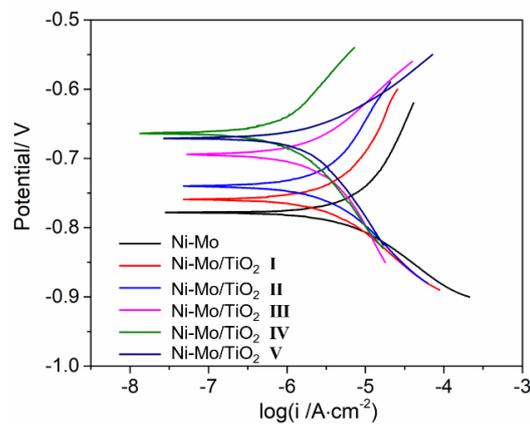

Figure 4. Polarization curves of the obtained Ni-Mo coating and Ni-Mo/TiO$_2$ coatings in the 3.5 wt.% NaCl solution.

Fig. 3 shows the surface morphologies of the deposited coatings, which are obviously influenced by the addition of TiO_2 nanoparticles. All the obtained coatings are compact and crack-free. Furthermore, the coatings deposited in the bath without TiO_2 nanoparticles exhibit a cauliflower-like appearance, which is composed of compact fine grains. This cauliflower-like characteristic of a coating from a bath containing TiO_2 nanoparticles becomes less obvious, and the coating becomes more uniform with an increased addition of TiO_2 nanoparticles. This may be because the TiO_2 nanoparticles provide nucleated active sites and reduce the orientation of the (111) grains (shown in Fig. 2). However, irregular agglomeration is observed in the Ni-Mo/TiO2 V nanocomposite coating (the addition of TiO_2 nanoparticles is 50 mg/L) due to an unavoidable agglomeration in the bath containing a high concentration of nanoparticles at a relatively high temperature (60 °C in this paper).

Table 1. E_{corr} and i_{corr} values extrapolated from the polarization curves

Samples	E_{corr} (V)	I_{corr} ($\mu A/cm^2$)
Ni-Mo	-0.778	4.23
Ni-Mo/TiO$_2$ I	-0.758	2.25
Ni-Mo/TiO$_2$ II	-0.740	1.78
Ni-Mo/TiO$_2$ III	-0.706	1.04
Ni-Mo/TiO$_2$ IV	-0.663	0.52
Ni-Mo/TiO$_2$ V	-0.671	0.99

Fig. 4 displays the polarization curves of the Ni-Mo and Ni-Mo/TiO$_2$ nanocomposite coatings. Extrapolated electrochemical parameters are displayed in Table 1. Obviously, the obtained Ni-Mo/TiO$_2$ nanocomposite coatings exhibit much greater E_{corr} and lower corrosion current density (i_{corr}) than those of the Ni-Mo alloy coating, indicating that the obtained Ni-Mo/TiO$_2$ nanocomposite coatings possess much better performance in general corrosion resistance [34, 35]. In addition, the i_{corr} decreased with an increasing addition of TiO_2 nanoparticles from 10 mg/L to 40 mg/L due to an increase in Mo content in the coating and the improvement of the morphological surface quality. However, there is a slight increase in i_{corr} when the addition of TiO_2 nanoparticles continues to increase to 50 mg/L (Ni-Mo/TiO$_2$ V nanocomposite coating) because of the inhomogeneous surface caused by agglomeration of the TiO_2 nanoparticles. This means that the Ni-Mo/TiO$_2$ nanocomposite coating deposited from a bath containing 40 mg/L possesses the optimal corrosion resistance.
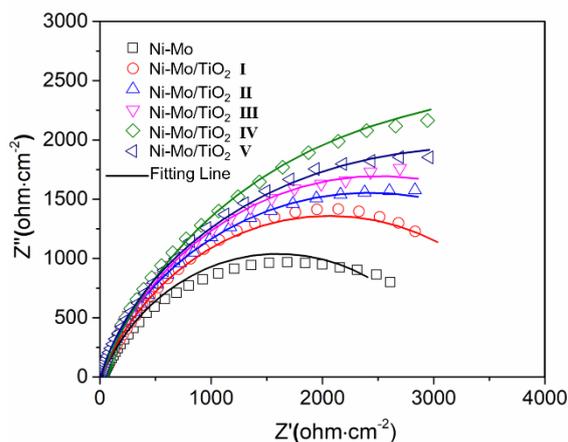
Figure 5. Nyquist plots of the obtained Ni-Mo coating and Ni-Mo-TiO$_2$ coatings in the 3.5 wt.% NaCl solution.

EIS was employed to investigate the corrosion behaviours at the electrolyte/obtained coating interface. Moreover, a simple electrical equivalent circuit (EEC, where R_s represents the solution resistance, Q stands for the constant phase element (CPE) of the electrical double layer (EDL), and R_{ct} is the charge transfer resistance) was used to fit the EIS plots (Fig. 6), and the results are listed in Table 2 [36, 37]. As shown in the Nyquist plots (Fig. 5), the fitted lines are quite close to the experimental data, and the chi-square values (Table 2) are very small (<10^{-3}, in orders of magnitude), confirming the good fit. Clearly, the values of R_{ct} of the Ni-Mo/TiO$_2$ nanocomposite coatings are much larger than that of the Ni-Mo alloy coating. Among all the obtained coatings, the Ni-Mo/TiO$_2$ IV nanocomposite coating shows the best corrosion resistance (the largest R_{ct} value). These results are correspond well with the conclusion obtained from the polarization curve analysis.
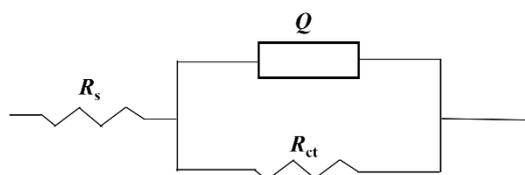

Figure 6. EEC for fitting the EIS experimental data.

Table 2. Equivalent circuit parameters for the impedance spectra of the obtained coatings

Samples	R_S (Ω cm^2)	Q_c (10^{-5} Ω^{-1} cm^{-2} s^n)	n_c	R_c (kΩ cm^2)	Σc^2
Ni-Mo	17.33	2.63	0.74	3.18	8.34×10^{-4}
Ni-Mo/TiO$_2$ I	10.73	4.47	0.76	3.89	6.72×10^{-4}
Ni-Mo/TiO$_2$ II	11.25	7.24	0.80	4.13	1.96×10^{-4}
Ni-Mo/TiO$_2$ III	10.55	7.69	0.79	4.58	3.77×10^{-4}
Ni-Mo/TiO$_2$ IV	11.39	8.90	0.81	6.55	2.58×10^{-4}
Ni-Mo/TiO$_2$ V	10.58	8.12	0.75	5.57	3.93×10^{-4}

4. CONCLUSIONS

In this paper, Ni-Mo/TiO$_2$ nanocomposite coatings were successfully deposited on the surface of low-carbon steel from a modified ammonia-citrate bath containing different additions of TiO$_2$ nanoparticles. The following conclusions can be drawn from the results discussed above.

(1) The Ni-Mo/TiO$_2$ nanocomposite coatings are composed of a Ni-Mo alloy matrix and a TiO$_2$ phase. Both the content of Mo and TiO$_2$ in the composite coating increased with an increasing addition of TiO$_2$ nanoparticles in the bath.

(2) The Ni-Mo/TiO$_2$ nanocomposite coatings are compact and crack-free. A cauliflower-like characteristic of the coating become less obvious, and the coating becomes more uniform with an increased addition of TiO$_2$ nanoparticles as long as the addition is no more than 40 mg/L; Otherwise, irregular agglomeration is observed in the Ni-Mo/TiO$_2$ V nanocomposite coating, which is from the bath with 50 mg/L TiO$_2$ nanoparticles.

(3) The obtained Ni-Mo/TiO$_2$ nanocomposite coatings exhibit much greater E_{corr}, lower i_{corr} and larger R_{ct} values than those of the Ni-Mo alloy coating. Among all coatings, the Ni-Mo/TiO$_2$ IV nanocomposite coating shows the best corrosion resistance.

References

1. S. Ding, T. Xiang, C. Li, S. Zheng, J. Wang, M. Zhang, C. Dong and W. Chan, *Mater. Des.*, 117 (2017) 280.
2. A. Liang, Y. Li, H. Liang, N. Liwei and Z. Junyan, *Mater. Lett.*,189 (2017) 221-224.
3. V. S. Helbert, M. Dhondt, R. Homette, S. A. Chirani and S. Calloch, *Mater. Res. Express.*, 5 (2018) 036522.
4. H. Zhang, L. Liu, J. Bai and X. Liu, *Thin Solid Films*,595 (2015) 36-40.
5. P. Lima-Neto, A. N. Correia, G. L. Vaz, P. N. S. Casciano, *J. Braz. Chem. Soc.*, 21 (2010) 10,1968-1976.
6. Q. Zhou, W. Xie, Y. Zhang, L. Qi and X. Wang, *J. Mater. Eng. Perform.*, 6 (2017) 2465-2471.
7. X. Meng, X. Shi, Q. Zhong, M. Shu and G. Xu, *J. Mater. Eng. Perform.*,11 (2016) 4735-4740.
8. Q. Zhou, W. Xie, Y. Zhang, M. Sheng, A. Hu, X. Cheng And L. Zhang, *Surf. Rev. Lett.*, 24 (2017) 1850015.
9. R. Abdel-Karim, J. Halim, S. El-Raghy, M. Nabil and A. Waheed, *J. Alloys Compd.*, 530 (2012) 85-90.
10. J. Winiarski, W. Tylus, B. Szczygieł., *Appl. Surf. Sci.*, 364 (2016) 455-466.
11. J. Füzer, P. Kollár, D. Olekšáková and S. Roth, *J. Alloys Compd.*, 483 (2009) 557-559.
12. A. Laszczyńska, J. Winiarski, B. Szczygieł, I. Szczygieł, *Appl. Surf. Sci.*, 369 (2016) 224-231.
13. A. Rezaeiolum, M. Aliofkhazraei, A. Karimzadeh, A. S. Rouhaghdam and R. Miresmaeili, *Surf. Eng.*, 34(2018): 423-432.
14. Y. H. Ahmad, J. Tientong, M. Nar, N. D'Souza, A. M. A. Mohamed and T. D. Golden, *Surf. Coat. Technol.*, 259 (2014) 517-525.
15. Y. Zhang, X. Leng, X. Wang, P. Ou, W. Zhang, Q. Zhou, *Metallogr. Microstruct. Anal.* 6 (2017) 519-

526.
16. B. M. Praveen, T. V. Venkatesha, Ap*pl. Surf. Sci.*, 254 (2008), 2418-2424.
17. Q. Li, X. Yang, L. Zhang, J. Wang and B. Chen, *J. Alloys Compd*. 482 (2009) 339-344.
18. X. K. Yang, Q. Li, S. Y. Zhang, X. K. Zhong, Y. Dai and F. Luo, *Mater. Corros.*, 61 (2010) 618-625.
19. K. A. Kumar, G. P. Kalaignan, V. S. Muralidharan, *Ceram. Int.*, 39 (2013) 2827-2834.
20. H. H. Sheu, J. H. Syu, Y. M. Liu, K. H. Hou and M. D. Ger, *Int. J. Electrochem. Sci*., 13 (2018) 3267-3278.
21. Q. Zhou, Y. Wang, H. Wu, Q. Zhong and J. Jiang, *Surf. Coat. Technol.*, 207 (2012) 503-507.
22. S. Zhang, Y. Li, C. Wang and X. Zhao, *Int. J. Electrochem. Sci.*, 14 (2019) 91-101.
23. B. Li, W. Zhang, Y. Huan and J. Dong, *Surf. Coat. Technol*., 337(2018) 186-197.
24. M. Sheng, W. Weng, Y. Wang, Q. Wu and S. Hou, *J. Alloys Compd*.,743 (2018) 682-690.
25. V. Niksefat, M. Ghorbani, *J. Alloys Compd*., 633 (2015) 127-136.
26. E. Beltowska-Lehman, A. Bigos, P. Indyka and M. Kot, *Surf. Coat. Technol*., 211 (2012) 67-71.
27. R. Mousavi, M. E. Bahrololoom, F. Deflorian and L. Ecco, *Appl. Surf. Sci*., 364 (2016) 9-14.
28. U. P. Kumar, C. J. Kennady and Q. Zhou, *Surf. Coat. Technol*., 283 (2015) 148-155.
29. J Shen, H. Wang, Y. Song, Y. Zhou, N. Ye, L. Fang and L. Wang, *Chem. Eng. J.* 240 (2014) 379-386.
30. Y. Wang, Q. Zhou, K. Li, Q. Zhong and Q. Bui., *Ceram. Int.*, 1 (2015) 79-84.
31. W. Tu, B. Xu, S. Dong and H. Wang, *Mater. Lett.*, 60 (2006) 1247-1250.
32. R. Mousavi, M. E. Bahrololoom and F. Deflorian*, Mater. Des.,* 110 (2016) 456-465.
33. B. Li, W.Zhang, *Int. J. Electrochem. Sci*., 8 (2017) 7017-7030.
34. F. Czerwinski, J. A. Szpunar, *Nanostruct. Mater.*, 5 (1999) 669-676.
35. Q. Zhou, S. Sheikh, P. Ou, D. Chen, Q. Hu and S. Guo, *Electrochem. Commun.*, 98 (2019) 63-68.
36. D. Zhang, H. Qian, L. Wang and X. Li*, Corros. Sci.*, 103 (2016) 230-241.
37. Q. Zhou, J. Jiang, Q. Zhong, Y. Wang, K. Li and H. Liu, *J. Alloys Compd*., 563(2013) 171-175.